Materials Science-Poland, 39(4), 2021, pp. 545-554
http://www.materialsscience.pwr.wroc.pl/
DOI: 10.2478/msp-2021-0047

Influence of spray distance on mechanical and tribological properties of HVOF sprayed WC-Co-Cr coatings

Monika Górnik[1], Ewa Jonda[2], Leszek Łatka[1,*], Monika Nowakowska[1], Marcin Godzierz[3]

[1]Department of Metal Forming, Welding and Metrology, Faculty of Mechanical Engineering, Wroclaw University of Science and Technology, 5 Łukasiewicza Str., 50371 Wroclaw, Poland

[2]Department of Engineering Materials and Biomaterials, Silesian University of Technology, 18a Konarskiego Str., 44100 Gliwice, Poland

[3]Centre of Polymer and Carbon Materials Polish Academy of Sciences, 34 M. Curie-Skłodowskiej Str., 41819 Zabrze, Poland

In this work, the tungsten carbide reinforcement in cobalt matrix (WC-Co-Cr) coatings was studied. The deposition process was carried out by high-velocity oxy-fuel spraying (HVOF). The study aimed to investigate the influence of one of the key process parameters, namely spray distance, on the coatings' microstructure and phase composition, as well as their mechanical and tribological properties. The manufactured coatings were analysed by scanning electron microscopy, X-ray diffraction (XRD), instrumented indentation test, pull-off adhesion test and ball-on-disc method. The results revealed that selection of proper spray distance caused a high index of carbide retention (ICR) amounting to 0.95, which promoted higher hardness and better wear resistance. Instrumental microhardness was in the range of 14.2–14.8 GPa, whereas the Young modulus exhibited values from 336 GPa up to 342 GPa. The bond strength of deposited coatings was in the range of 55–65 MPa. Wear factor values were in the range of 73–81 $\times$ 10^{-7} $mm^3/(N \cdot m)$ and the friction coefficient was about 0.4. The dominant wear mechanism is abrasion and adhesive mode supported by the fatigue-induced material delamination.

Keywords: *high-velocity oxy-fuel spraying, cermet coatings, mechanical properties, phase analysis, wear resistance*

1. Introduction

In the field of surface engineering, thermal spraying is a well-known technique employed in order to deposit various types of protective coatings that are used in a wide range of industrial branches [1–3]. Depending on the application, different coating manufacturing processes could be selected: flame [4, 5], arc [6, 7], plasma [8, 9] or cold spray [10, 11]. Among them, high-velocity oxy-fuel spraying (HVOF) is the primary method used to deposit hard, wear-resistant coating that exhibits both corrosion and erosion resistance [12, 13]. In this technique, gas combustion is used as an energy source that melts and accelerates powder particles.

Construction of the gun enables in-flight particles to achieve supersonic velocity (up to 2,000 m/s). On the other hand, the flame temperature is much lower than for plasma jet (c.a. 3,500 K instead of c.a. 15,000 K) [14]. These conditions make it possible to obtain coatings with very low porosity levels and low oxidation factors, as well as high adhesion to the substrate [15, 16]. Moreover, this method allows depositing both ceramic and metallic coatings, as well as cermet ones [17–19]. In addition, even polymers could be deposited by the HVOF technique, but it requires a very short residence time in the flame. Such coatings are used in dry sliding wear [20]. Nevertheless, among all the material types, the most frequently used is cermet. An additional advantage of thermal spraying is the possibility of replacement electrolytic hard chromium plating (EHC). This technology is considered environmentally hazardous, especially in industrial-scale applications [21, 22].

In general, manufactured coatings derived from the hard metals and their composites are used in extreme work conditions, e.g. impeller shafts, conveyor screws, pump housings etc. [14]. One of the most commonly used feedstock materials in the

* E-mail: leszek.latka@pwr.edu.pl

© 2021. This is an open access article distributed under the Creative Commons Attribution-NonCommercial-NoDerivatives 4.0 License. (http://creativecommons.org/licenses/by-nc-nd/4.0/)

HVOF process is WC-Co, or wider, WC-based cermet. Such materials demonstrate very good wear resistance [23]. The most fundamental types of feedstock are WC-12 wt% Co, WC-17 wt% Co and WC-12 wt% Ni. These coatings have been intensively investigated for many years [24–26]. Development of different industry branches forced researchers to search for materials exhibiting improved properties. Among others, the addition of chromium to the cobalt matrix was found to improve the wear resistance of deposited coatings [27]. Nevertheless, it requires adjusting the appropriate process parameters, as well as the adequate chromium content. Among many parameters that strongly influence the quality and properties of manufactured coatings, spray distance is one of the key parameters. Moreover, during industrial conditions, this factor can be changed most easily, in contrast to e.g. gas flow rate [28, 29].

In this work, WC-Co-Cr (with 10 wt% Co and 4 wt% Cr) coatings manufactured by HVOF with different spray distances were characterised in terms of their microstructure, phase composition and mechanical and tribological properties, including adhesion, microhardness and sliding wear resistance. So far, the influence of spray distance in WC-Co-Cr coatings has been investigated only in a small number of articles. Such research has been carried out e.g. by Hong et al. [30], Lee and Kim [31] and Gui et al. [32].

2. Materials and methods

The feedstock material used in the current investigation was a commercial powder of tungsten carbide with the addition of chromium in cobalt matrix (Amperit 554.071 by Hoganas). The nominal chemical composition was (in wt%) WC – 86, Co – 10 and Cr – 4. The morphology of the initial powder is presented in Figure 1. The powder particles were sintered and it was ensured that the particle size did not exceed 60 µm, according to the manufacturer's instructions. Own measurements of the particle size distribution (PSA 1090, Anton Paar, Graz, Austria) confirmed this, and the mean volume to surface diameter (d_{VS50}) was 16 µm.

Coupons of mild steel S235JR, with thickness 3 mm and diameter 25 mm, were used as the substrate material. Before spraying, the substrate surface was degreased and sand-blasted under a pressure of 0.6 MPa using alumina powder (mesh 40). The roughness of the substrate surface was determined using a MarSurf PS10 profilometer (Mahr, Esslingen, Germany) as an average of five measurements. Just before the deposition process, the substrates were cleaned using an ultrasonic bath.

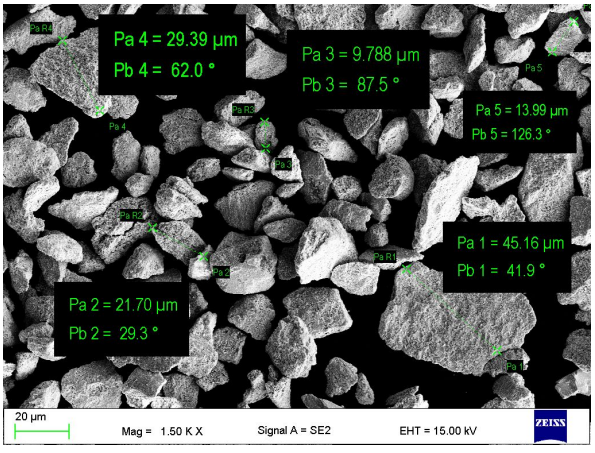


Fig. 1. Morphology of initial feedstock power (SEM-SE) with random measurements of particle size. SEM, scanning electron microscope

Cermet coatings were sprayed using a CJS K5.2 N (Thermico) gun in the HVOF method. The scheme of the deposition process is presented in Figure 2. The powder feed rate was 30 g/min and it was delivered by a carrier gas (nitrogen) with a flow rate of 12 l/min. Flow rates for fuel media were as follows: kerosene – 16 l/h, oxygen – 600 l/min and hydrogen – 100 l/min. Linear gun velocity was 800 mm/s. The sample code and values of spray distance are collected in Table 1.

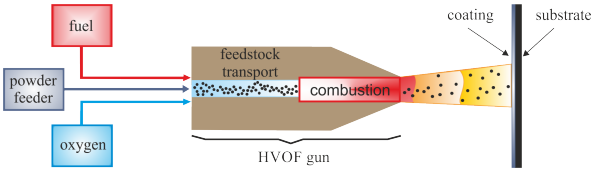


Fig. 2. Schematic representation of the HVOF method and its key process parameter, inspired by Pawłowski [3] and Jonda and Łatka [33]. HVOF, high-velocity oxy-fuel spraying

Table 1. Values of spray distance and sample code

Sample code	**A1**	**A2**	**A3**
Spray distance, mm	240	280	320

The metallographic samples were prepared by a standard procedure, which is as follows: samples were mechanically cut, embedded in epoxy resin and then ground and polished. The microstructure of manufactured coatings was analysed using a scanning electron microscope (SEM), Tescan Vega 3 (Tescan Orsay Holding).

The porosity of deposited coatings was analysed using ImageJ open source software (1.50i version). For each sample, 20 images were taken at a magnification of 1,000×. These images also have been obtained using SEM.

X-ray diffraction (XRD) investigations were performed using the D8 Advance diffractometer (Bruker, Karlsruhe, Germany). The set-up was equipped with a Cu-K_α cathode (with wavelength λ = 0.154 nm). The operating parameters were 40 kV for voltage and 40 mA for current. XRD characterisation was performed in the range of 2θ from 20° up to 120°, with a scanning step and scan rate of 0.02° and 0.60°/min, respectively. The DIFFRAC.EVA programme equipped with the ICDD PDF#2 database was used to identify fitted phases. Instrumental indentation tests were performed with a Nanondenter NHT^3 (Anton Paar, Graz, Austria) equipped with a Berkovich diamond indenter. For instrumental hardness estimation, the values of maximum load and dwell time were 500 mN and 15 s, respectively. This procedure is based on the original methodology proposed by Oliver and Phar [34]. On the other hand, to determine the instrumented elastic modulus (EIT), different values of the maximum load were used, in a range of 50–500 mN. Details about this methodology can be found in Łatka et al. [35].

The pull-off adhesion test was carried out using an Elcometer 510 tester (Elcometer Instruments, Manchester, UK), according to the ISO 14916 standard. The samples were glued to the counter-surface with cold cure epoxy adhesive Epidian 53, with a theoretical strength of 70 MPa. Pins having a diameter of 10 mm and a load rate of 0.4 MPa/s were used during testing.

The dry sliding wear tests were carried out using the 'pin-on-disc' method in accordance with the ASTM G99 standard with a linear mode tribometer, version 6.1.19 (Anton Paar, Peseux, Switzerland). Before tests, coatings were ground and polished in order to obtain a surface roughness (R_a) below 0.8 μm (according to standard requirements). As a counter-body, a sintered and polished alumina ball with a diameter of 6 mm was used. The tests were performed under ambient conditions over a distance of 1,000 m, and the relative sliding speed and the normal load were 0.1 m/s and 10 N, respectively. The volume loss of coatings was determined by stylus profilometry (Surtronic 25, Taylor Hobson, Leicester, UK). The wear rate (K_V) was calculated from the wear formula proposed by Lancaster [36].

3. Experimental results and discussion

3.1. Microstructure and phase composition

An example of a sprayed surface topography is presented in Figure 3. Some irregularly shaped WC grains can be observed. This is a result of melting of the matrix during flying in the flame. On the other hand, WC grains with a high melting point were not dissolved in the flame [37, 38].

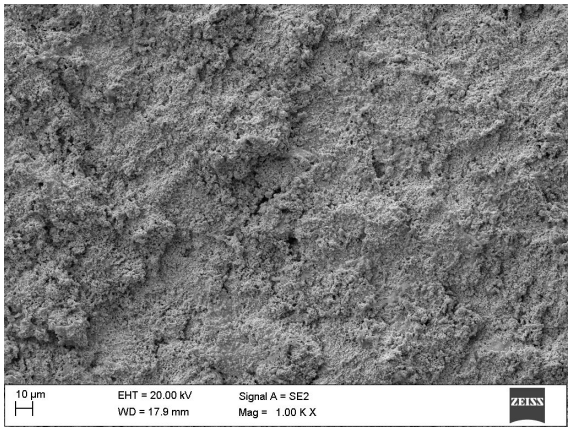


Fig. 3. The topography of the A1 sample surface

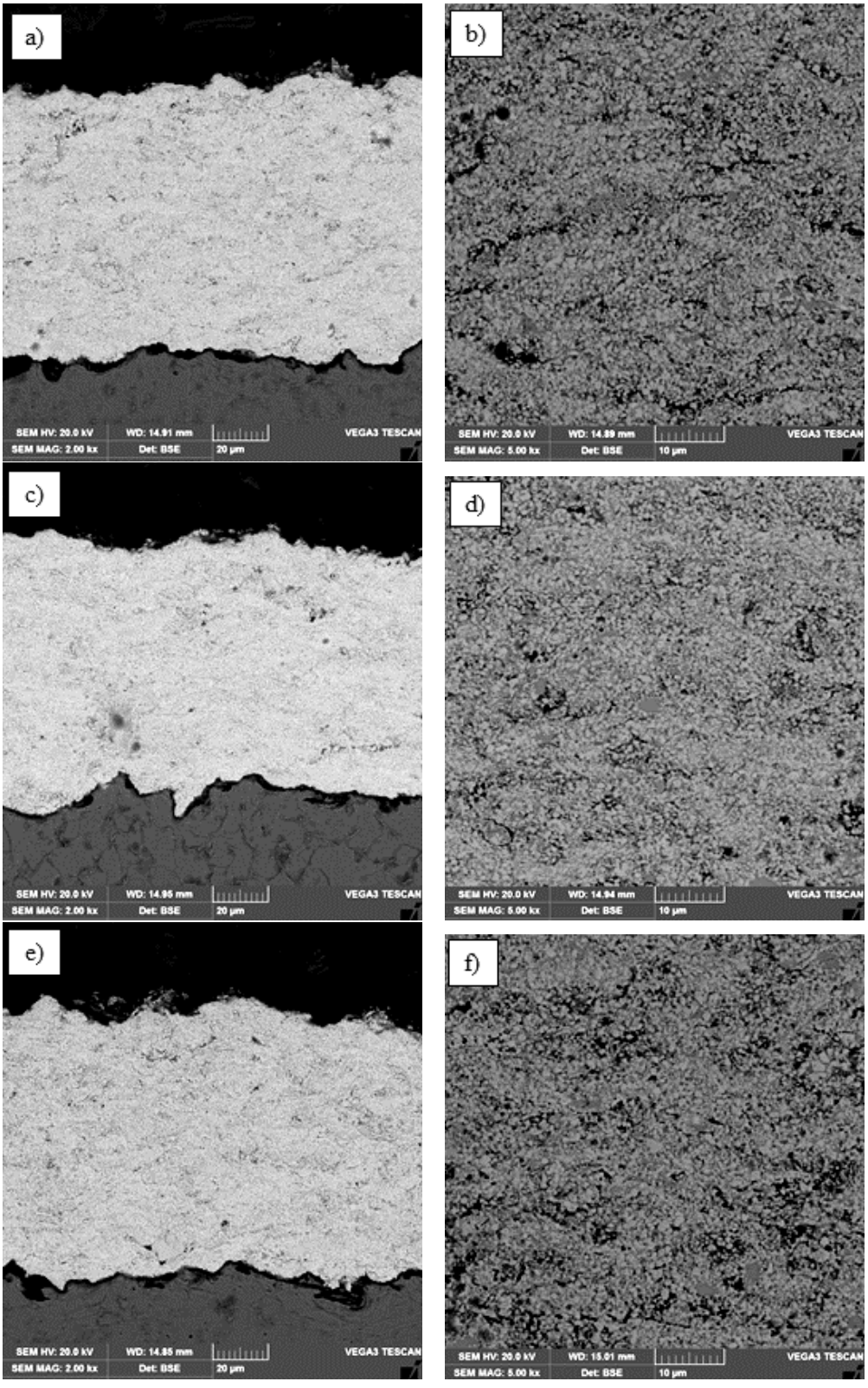


Fig. 4. SEM images of coatings' cross sections: **(A, B)** sample A1; **(C, D)** sample A2; **(E, F)** sample A3; **(A, C, E)** – mag. 2,000×; **(B, D, F)** – mag. 5,000×. SEM, scanning electron microscope

The microscopic observation of coatings of all cross sections revealed a relatively smooth and dense structure (Figure 4 left column). Such compact and uniform structure results from inherent features of the HVOF method (high kinetic energy of the particles). Moreover, it could be observed that at the coating–substrate interface, the coating material had filled the unevenness of the substrate surface, and good interlocking with the substrate had occurred [39–41]. All coatings have been deposited in order to obtain c.a. 100 μm in thickness.

Detailed examination at higher magnifications (Figure 4 right column) shows a low level of porosity with fine pores, whose size is lower than 3 μm. The calculated porosity of A1, A2 and A3 coatings is 2.5 ± 0.4, 3.3 ± 0.6 and 3.9 ± 0.7, respectively. Similar results have been obtained in the literature [42, 43]. It should be stressed that similar results of coatings porosity for the same material and with nearing spray distance were obtained by Murugan et al. [44].

Phase compositions of the deposited coatings are presented in Figure 5. In all coatings, hexagonal WC (PDF#00-061-0244) was the main phase. The second phase, hexagonal W_2C carbide (PDF#00-035-0776), appeared. Thus, it is evident that during coating deposition, partial decarburisation of WC has taken place. It is a well-known mechanism for tungsten carbide coatings [45, 46].

On the other hand, Cr addition to WC-Co slows down the decarburisation of WC. Moreover, Cr reinforces the cobalt matrix in the binding function of WC grains [47]. The last phase identified was a cubic solid solution of tungsten in cobalt with composition $Co_{0.9}W_{0.1}$ (PDF#03-065-9928). The index of carbide retention (ICR) has been proposed by Bartuli et al. [48] as a tool with which to determine the influence of process parameters on the degree of coatings' decarburisation. This indicator compares the intensity of the (100) peak of WC at 2θ = 35.6° and the intensity of the (101) peak of W_2C at 2θ = 39.6° according to Eq. (1):

$$ICR = \frac{I_{WC}}{I_{WC} + I_{W_2C}} \tag{1}$$

For coating A1, the ICR value is 0.93 whereas it is 0.95 for coatings A2 and A3. These values are similar to those of Picas et al. [49]. In general, values of ICR closer to unity are better, because the formation of W_2C phase, which exhibits lower hardness, is more difficult [50].

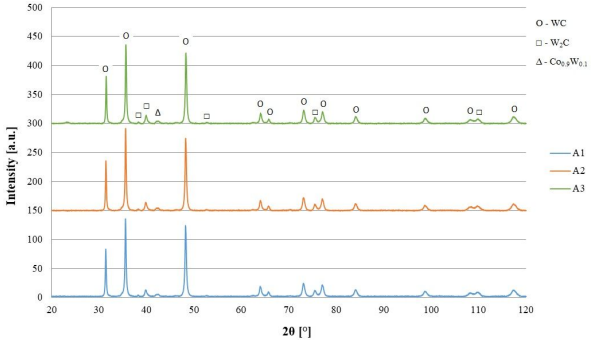


Fig. 5. XRD patterns of all WC-Co-Cr coatings manufactured by the HVOF method. XRD, X-ray diffraction; HVOF, high-velocity oxy-fuel spraying

3.2. Mechanical properties

Measurements of hardness instrumented indentation (HIT) revealed a slight influence of spray distance (Table 2). All coatings are characterised by hardness values between 14 GPa and 15 GPa and the values are not significantly different within the error range. These results are comparable with the results of other investigations [19, 51]. In the case of elastic modulus, it could be noted that the low-

Table 2. Values of elastic modulus and hardness from instrumental indentation test

	A1	A2	A3
HIT, GPa	14.82 ± 1.25	14.67 ± 1.55	14.24 ± 1.35
EIT, GPa	339	342	336

Table 3. Mean values of bond strength and type of fracture

	A1	A2	A3
Bond strength, MPa	65 ± 3	61 ± 4	55 ± 3
Fracture type	A/C	A/C	A/C

A/C, adhesive-cohesive type of fracture

Table 4. Sliding wear results: wear factor and friction coefficient (CoF)

	A1	**A2**	**A3**
K, 10^{-9} mm^3/(N · m)	77 ± 11	73 ± 9	81 ± 14
CoF, -	0.41 ± 0.07	0.40 ± 0.09	0.40 ± 0.07

est EIT value is connected with the longest spray distance. For other samples, there is no such visible tendency and the obtained results are consistent with the literature [52, 53].

The tensile adhesion tests were carried out to estimate bond strength. The results are shown in Table 3. The influence of spray distance is visible from the results. However, the differences between values are only a little more than the limits of the standard deviation. Such results are comparable with the literature [54, 55]. For all samples fracture type was an adhesive-cohesive one.

3.2.1. Tribological properties

The results of dry sliding wear investigations in form of wear factor are given in Table 4. The obtained results confirmed that the deposited coatings exhibit very good wear resistance. Moreover, the slight influence of spray distance is also observed. Similar results can be found in the literature [41, 51, 56].

In order to understand the wear mechanism, the worn surfaces of investigated samples were examined by SEM. The wear traces of tested samples are presented in Figure 6. Identification of wear mechanism and occurred phenomena should take into account, that it is affected by two phases structure of cermet materials (hard grains and soft matrix). On the other hand, the wear resistance of HVOF sprayed coatings depends on many factors, e.g. microstructure, hardness, cohesion in the coating and porosity level [57]. The detailed analysis of wear traces of the tested coatings leads to the conclusion that two types of mechanism occurred: (i) subsurface plastic deformation and (ii) brittle cracking [51]. It should be stressed that these two mechanisms occur simultaneously. Due to the friction between two bodies, shear stresses occur, which makes possible the plastic flow of the soft metal matrix. On the other hand, during the brit-

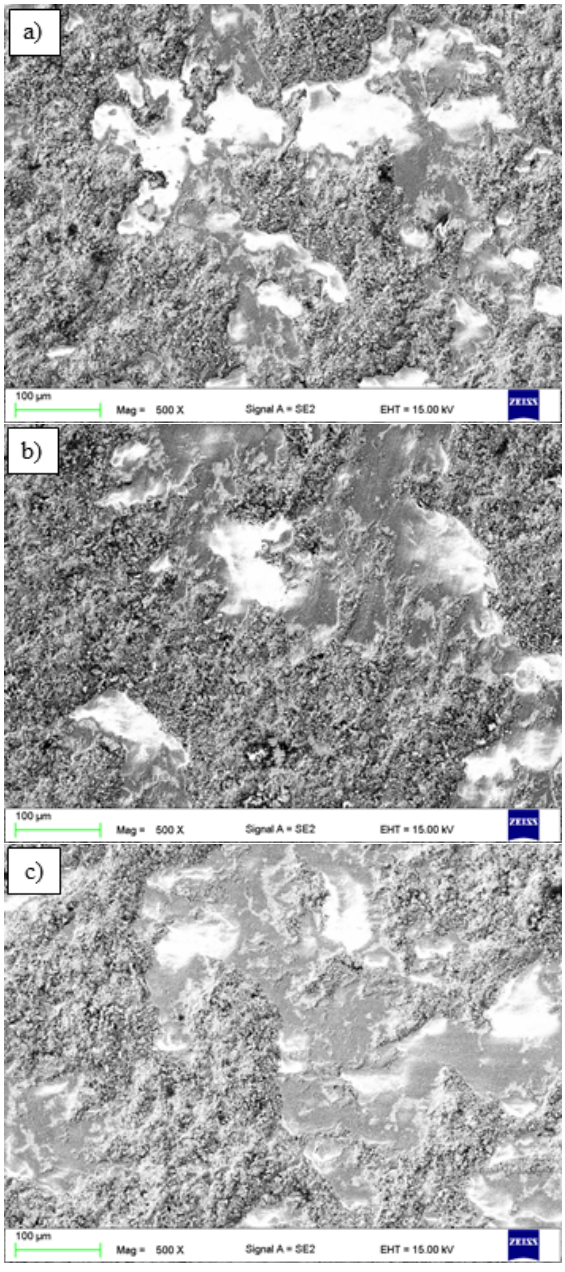


Fig. 6. SEM images showing the wear track of deposited coatings: **(A)** A1, **(B)** A2, **(C)** A3. SEM, scanning electron microscope

tle cracking, coating material detachment has occurred. Mainly, hard carbides particles are removed [58]. In all samples, the specific friction layer is built on their surface (Figure 6).

It contains mixed ingredients of the coating material (darker smooth areas) and less densely compacted wear debris, which are also oxidated (bright smooth areas) due to an increasing temperature during the test [59, 60].

Summarising all the conducted investigations and their results, some recommendations related to specific areas of application can be provided. In general, a shorter spray distance is recommended for applications that require improved corrosion resistance as it is connected with low porosity and a more homogenous structure. A slightly higher spray distance could be recommended for applications where good wear and erosion resistance are important. Too short a spray distance results in breaking the powder particles instead locking in surface unevenness. Moreover, for cermet materials, an excessive melting of carbides could take place. On the other hand, too long a spray distance leads to a reduction in velocity and insufficient particle deformation. In both cases, the porosity level significantly increases.

4. Conclusions

In this paper, HVOF spraying with cermet feedstock powder having the chemical composition WC-10Co-4Cr was carried out. The coatings were studied in terms of the influence of spray distance on the microstructure and phase composition, as well as mechanical and tribological properties. The following findings are summarised:

1. All coatings were successfully deposited; moreover, in each sample, the interface between coating and substrate was clear. There was no evidence of delamination or other discontinuities.
2. SEM micrographs revealed dense, compact and homogenous structure with a relatively low level of porosity, in the range 2.5–3.9 vol.%.
3. XRD phase analysis revealed the presence of hexagonal WC, hexagonal W_2C carbide and a cubic solid solution of tungsten in cobalt with the composition $Co_{0.9}W_{0.1}$. Moreover, longer spray distances result in a slightly higher ICR (ICR = 0.95) instead of 0.93 for the shortest spray distance.
4. Instrumental indentation hardness (HIT) shows a clear tendency with spray distance, which is as follows: $HIT_{A1} > HIT_{A2} > HIT_{A3}$. All values are in the range between 14 GPa and 15 GPa. On the other hand, the instrumental elastic modulus (EIT) could be related with spray distance and amount of WC phase (improvement in stiffness). EIT values for deposited coatings were 339 GPa, 342 GPa and 336 GPa for A1, A2 and A3 samples, respectively.
5. The main tensile adhesion of all coatings to the substrate was 65 MPa, 61 MPa and 55 MPa for A1, A2 and A3 samples, respectively. It is connected with the coating porosity and very good mechanical interlock between coating and substrate.
6. The wear rate for all HVOF coatings did not exceed the level of 10^{-7} $mm^3/(N \cdot m)$. The best wear resistance has been achieved for sample A2 (average spray distance) and it was probably caused by a beneficial mix of compact structure, high hardness and stiffness and high ICR (0.95). The CoF value (approximately 0.4 for all samples) indicates that no seizure occurs between the surfaces that are in contact. The wear mechanism includes plastic deformation and brittle cracking.

Acknowledgements

The authors gratefully acknowledge Certech Company in Wilamowice, Poland, for help in the coating deposition process.

References

[1] Dwivedi DK. Surface engineering: Enhancing life of tribological components. Springer; 2018.
[2] Heimann RB. Plasma-spray coating: Principles and applications. 2nd ed. John Wiley & Sons; 2008.

[3] Pawłowski L. The science and engineering of thermal spray coatings. 2nd ed. John Wiley & Sons; 2008

[4] Donadei V, Koivoluoto H, Sarlin E, Vuoristo P. Lubricated icephobic coatings prepared by flame spraying with hybrid feedstock injection. Surf Coat Tech. 2020;403:126396. https://doi.org/10.1016/j.surfcoat.2020.126396.

[5] Czupryński A. Flame spraying of aluminum coatings reinforced with particles of carbonaceous materials as an alternative for laser cladding technologies. Materials. 2019;12:3467. https://doi.org/10.3390/ma12213467.

[6] Devaraj S, McDonald A, Chandra S. Metallization of porous polyethylene using a wire-arc spray process for heat transfer applications. J Therm Spray Techn. 2021;30:145–56. https://doi.org/10.1007/s11666-020-01119-1.

[7] Chmielewski T, Siwek P, Chmielewski M, Piątkowska A, Grabias A, Golański D. Structure and selected properties of arc sprayed coatings containing in-situ fabricated Fe-Al intermetallic phases. Metals. 2018;8:1059. https://doi.org/10.3390/met8121059.

[8] de la Roche J, Alvarado-Orozco JM, Gomez PA, Cano IG, Dosta S, Toro A. Hot corrosion behavior of dense CYSZ/YSZ bilayer coatings deposited by atmospheric plasma spray in Na2SO4 + V2O5 molten salts. Surf Coat Tech. 2022;432:128066. https://doi.org/10.1016/j.surfcoat.2021.128066.

[9] Łatka L, Michalak M, Szala M, Walczak M, Sokołowski P, Ambroziak A. Influence of 13 wt% TiO2 content in alumina-titania powders on microstructure, sliding wear and cavitation erosion resistance of APS sprayed coatings. Surf Coat Tech. 2021;410:126979. https://doi.org/10.1016/j.surfcoat.2021.126979.

[10] Huang C, Arseenko M, Zhao L, Xie Y, Elsenberg A, Li W, et al. Property prediction and crack growth behavior in cold sprayed Cu deposits. Mater Design. 2021;206:109826. https://doi.org/10.1016/j.matdes.2021.109826.

[11] Winnicki M, Gibas A, Baszczuk A, Jasiorski M. Low pressure cold spraying of TiO2 on acrylonitrile butadiene styrene (ABS). Surf Coat Tech. 2021;406:126717. https://doi.org/10.1016/j.surfcoat.2020.126717.

[12] Singh V, Singh I, Bansal A, Omer A, Singla AK, Rampal A, Goyal DK. Cavitation erosion behavior of high velocity oxy fuel (HVOF) sprayed (VC + CuNi-Cr) based novel coatings on SS316 steel. Surf Coat Tech. 2022;432:128052. https://doi.org/10.1016/j.surfcoat.2021.128052.

[13] Praveen AS, Arjunan A. High-temperature oxidation and erosion of HVOF sprayed NiCrSiB/Al2O3 and NiCrSiB/WC–Co coatings. Appl Sur Sci Adv. 2022;7:100191. https://doi.org/10.1016/j.apsadv.2021.100191.

[14] Fauchais PL, Heberlein JVR, Boulos MI. Thermal spray fundamentals, from powder to part. Springer; 2014.

[15] Lima RS, Marple BR. Thermal spray coatings engineered from nanostructured ceramic agglomerated powders for structural, thermal barrier and biomedical applications: A review. J Therm Spray Techn. 2007;16:40–63. https://doi.org/10.1007/s11666-006-9010-7.

[16] Picas JA, Forn A, Matthaus G. HVOF coatings as an alternative to hard chrome for pistons and valves. Wear. 2006;261:477–84. https://doi.org/10.1016/j.wear.2005.12.005.

[17] Kiilakoski J, Langlade C, Koivuluoto H, Vuoristo P. Characterizing the micro-impact fatigue behavior of APS and HVOF sprayed ceramic coatings. Surf Coat Tech. 2019;371:245–54. https://doi.org/10.1016/j.surfcoat.2018.10.097.

[18] Mousavi SE, Naghshehkesh N, Amirnejad M, Shammakhi H, Sonboli A. Wear and corrosion properties of stellite-6 coating fabricated by HVOF on nickel–aluminium bronze substrate. Met Mater Int. 2020;27:3269–81. https://doi.org/10.1007/s12540-020-00697-7.

[19] Qiao L, Wu Y, Hong S, Long W, Cheng J. Wet abrasive wear behavior of WC-based cermet coatings prepared by HVOF spraying. Ceram Int. 2021;47:1829–36. https://doi.org/10.1016/j.ceramint.2020.09.009.

[20] Jackson L, Ivosevic M, Knight R, Cairncross RA. Sliding wear properties of HVOF thermally sprayed nylon-11 and nylon-11/ceramic composites on steel. J Therm Spray Technol. 2007;16:927–32. https://doi.org/10.1007/s11666-007-9088-6.

[21] Houdkova S, Zahalka F, Kasparova M, Berger L-M. Comparative study of thermally sprayed coatings under different types of wear conditions for hard chromium replacement. Tribol Lett. 2011;43:139–54. https://doi.org/10.1007/s11249-011-9791-9.

[22] Krelling AP, de Souza MM, da Costa CE, Giubilei Milan JC. HVOF-sprayed coating over AISI 4140 steel for hard chromium replacement. Mater Res. 2018;21:e20180138. https://doi.org/10.1590/1980-5373-MR-2018-0138.

[23] Berger L-M. Application of hardmetals as thermal spray coatings. Int J Refract Hard Met. 2015;49:350–64. https://doi.org/10.1016/j.ijrmhm.2014.09.029.

[24] Ma N, Guo L, Cheng Z, Wu H, Ye F, Zhang K. Improvement on mechanical properties and wear resistance of HVOF sprayed WC-12Co coatings by optimizing feedstock structure. Appl Surf Sci. 2014;320:364–71. https://doi.org/10.1016/j.apsusc.2014.09.081.

[25] Chen H, Gou GQ, Tu MJ, Liu Y. Structure and wear behaviour of nanostructured and ultrafine HVOF spraying WC-17Co coatings. Surface Eng. 2009;25:502–6. https://doi.org/10.1179/026708408X329489.

[26] Ward LP, Pilkington A. The dry sliding wear behavior of HVOF-sprayed WC: Metal composite coatings. J Mater Eng Perform. 2014;23:3266–78. https://doi.org/10.1007/s11665-014-1122-5.

[27] Murthy JKN, Venkataraman B. Abrasive wear behaviour of WC-CoCr and Cr3C2-20(NiCr) deposited by HVOF and detonation spray processes. Surf Coat Tech. 2006;200:2642–52. https://doi.org/10.1016/j.surfcoat.2004.10.136.

[28] Fang W, Cho TY, Yoon JH, Song KO, Hur SK, Youn SJ, et al. Processing optimization, surface properties and wear behavior of HVOF spraying WC–CrC–Ni coating. J Mater Process Tech. 2009;209:3561–7. https://doi.org/10.1016/j.jmatprotec.2008.08.024.

[29] Bang SS, Park YC, Lee JW, Hyun SK, Kim TB, Lee JK, et al. Effect of the spray distance on the properties of high velocity oxygen-fuel (HVOF) sprayed WC-12Co coatings. J Nanosci Nanotechnol. 2018;18:1931–4. https://doi.org/10.1166/jnn.2018.14990.

[30] Hong S, Wu Y, Zheng Y, Wang B, Gao W, Li G, et al. Effect of spray parameters on the corrosion behavior of HVOF sprayed WC-Co-Cr coatings. J Mater Eng Perform. 2014;23:1434–9. https://doi.org/10.1007/s11665-014-0865-3.

[31] Lee L, Kim S. Influence of thermally sprayed WC-Co-Cr coatings on the corrosion characteristics of Ni-Al bronze alloy. Int J Electrochem Sci. 2021;16:210769. https://doi.org/10.20964/2021.07.40.

[32] Gui M, Eybel R, Asselin B, Radhakrishnan S, Cerps J. Influence of processing parameters on residual stress of high velocity oxy-fuel thermally sprayed WC-Co-Cr coating. J Mater Eng Perform. 2012;21:2090–8. https://doi.org/10.1007/s11665-012-0134-2.

[33] Jonda E, Łatka L. Comparative analysis of mechanical properties of WC-based cermet coatings sprayed by HVOF onto AZ31 magnesium alloy substrates. Adv Sci Technol Res J. 2021;15:57–64. https://doi.org/10.12913/22998624/135979.

[34] Oliver WC, Pharr GM. An improved technique for determining hardness and elastic modulus using load and displacement sensing indentation experiments. J Mater Res. 1992;7:1564–83. https://doi.org/10.1557/JMR.1992.1564.

[35] Łatka L, Chicot D, Cattini A, Pawłowski L, Ambroziak A. Modeling of elastic modulus and hardness determination by indentation of porous yttria stabilized zirconia coatings. Surf Coat Technol. 2013;220:131–9. https://doi.org/10.1016/j.surfcoat.2012.07.025.

[36] Lancaster JK. The influence of substrate hardness on the formation and endurance of molybdenum disulphide films. Wear. 1967;10:103–17. https://doi.org/10.1016/0043-1648(67)90082-8.

[37] Aguero A, Camon F, Garcıa de Blas J, del Hoyo JC, Muelas R, Santaballa A, et al. HVOF-deposited WC-CoCr as replacement for hard Cr in landing gear actuators. J Therm Spray Techn. 2011;20:1292–309. https://doi.org/10.1007/s11666-011-9686-1.

[38] Ding X, Ke D, Yuan C, Ding Z, Cheng X. Microstructure and cavitation erosion resistance of HVOF deposited WC-Co coatings with different sized WC. Coatings. 2018;8:307. https://doi.org/10.3390/coatings8090307.

[39] Hong S, Wu Y, Wang B, Lin J. Improvement in tribological properties of Cr12MoV coldWork die steel by HVOF sprayed WC-Co-Cr cermet coatings. Coatings. 2019;9:825. https://doi.org/10.3390/coatings9120825.

[40] Wang H, Qiu Q, Gee M, Hou C, Liu X, Song X. Wear resistance enhancement of HVOF-sprayed WC-Co coating by complete densification of starting powder. Mater Des. 2020;191:108586. https://doi.org/10.1016/j.matdes.2020.108586.

[41] Song B, Murray JW, Wellman RG, Pala Z, Hussain T. Dry sliding wear behaviour of HVOF thermal sprayed WC-Co-Cr and WC-CrxCy-Ni coatings. Wear. 2020;442–443:203114. https://doi.org/10.1016/j.wear.2019.203114.

[42] Zhan S-H, Cho T-Y, Yoon J-H, Li M-X, Shum PW, Kwon S-C. Investigation on microstructure, surface properties and anti-wear performance of HVOF sprayed WC-Cr-Ni coatings modified by laser heat treatment. Mater Sci Eng B. 2009;162:127–34. https://doi.org/10.1016/j.mseb.2009.03.017.

[43] Yao H-L, Yang C, Yi D-L, Zhang M-X, Wang H-T, Chen Q-Y, et al. Microstructure and mechanical property of high velocity oxy-fuel sprayed WC-Cr3C2-Ni coatings. Surf Coat Tech. 2020;397:126010. https://doi.org/10.1016/j.surfcoat.2020.126010.

[44] Murugan K, Ragupathy A, Balasubramanian V, Sridhar K. Optimizing HVOF spray process parameters to attain minimum porosity and maximum hardness in WC-10Co-4Cr coatings. Surf Coat Tech. 2014;247:90–102. https://doi.org/10.1016/j.surfcoat.2014.03.022.

[45] Myalska H, Lusvarghi L, Bolelli G, Sassatelli P, Moskal G. Tribological behavior of WC-Co HVAF-sprayed composite coatings modified by nano-sized TiC addition. Surf Coat Tech. 2019;371:401–16. https://doi.org/10.1016/j.surfcoat.2018.09.017.

[46] Mateen A, Saha GC, Khan TI, Khalid F. Tribological behavior of HVOF sprayed near-nanostructured and microstructured WC-17wt.%Co coatings. Surf Coat Tech. 2011;206:1077–84. https://doi.org/10.1016/j.surfcoat.2011.07.075.

[47] Karimi A, Verdon Ch, Barbezat G. Microstructure and hydroabrasive wear behaviour of high velocity oxy-fuel thermally sprayed WC-Co(Cr) coatings. Surf Coat Tech. 1993;57:81–9. https://doi.org/10.1016/0257-8972(93)90340-T.

[48] Bartuli C, Valente T, Cipri F, Bemporad E, Tului M. Parametric study of an HVOF process for the deposition of nanostructured WC-Co coatings. J Therm Spray Techn. 2005;14:187–95. https://doi.org/10.1361/10599630523746.

[49] Picas JA, Ruperez E, Punset M, Forn A. Influence of HVOF spraying parameters on the corrosion resistance of WC–CoCr coatings in strong acidic environment. Surf Coat Tech. 2013;225:47–57. https://doi.org/

10.1016/j.surfcoat.2013.03.015.

[50] Bolelli G, Berger L-M, Borner T, Koivuluoto H, Lusvarghi L, Lyphout C, et al. Tribology of HVOF- and HVAF-sprayedWC–10Co4Cr hardmetal coatings: A comparative assessment. Surf Coat Tech. 2015;265:125–44. https://doi.org/10.1016/j.surfcoat.2015.01.048.

[51] Bolelli G, Berger L-M, Bonetti M, Lusvarghi L. Comparative study of the dry sliding wear behaviour of HVOF-sprayed WC–(W,Cr)2C–Ni and WC–CoCr hard metal coatings. Wear. 2014;309:96–111. https://doi.org/10.1016/j.wear.2013.11.001.

[52] Matikainen V, Peregrina SR, Ojala N, Koivuluoto H, Schubert J, Houdkova S, et al. Erosion wear performance of WC-10Co4Cr and Cr3C2-25NiCr coatings sprayed with high-velocity thermal spray processes. Surf Coat Tech. 2019;370:196–212. https://doi.org/10.1016/j.surfcoat.2019.04.067.

[53] Santana YY, La J, Barbera-Sosa G, Caro J, Puchi-Cabrera ES, Staia MH. Mechanical properties and microstructure of WC–10Co–4Cr and WC–12Co thermal spray coatings deposited by HVOF. Surf Eng. 2008;24:374–82. https://doi.org/10.1179/174329408X326380.

[54] Ang A, Berndt CC. A review of testing methods for thermal spray coatings. Int Mater Rev. 2014;59:179–223. https://doi.org/10.1179/1743280414Y.0000000029.

[55] Garfias Bulnes A, Albaladejo Fuentes V, Garcia Cano I, Dosta S. Understanding the influence of high velocity thermal spray techniques on the properties of different anti-wear WC-based coatings. Coatings. 2020;10:1157. https://doi.org/10.3390/coatings10121157.

[56] Wesmann JAR, Kuroda S, Espallargas N. The role of oxide tribofilms on friction and wear of different thermally sprayed WC-CoCr. J Therm Spray Technol. 2017;26:492–502. https://doi.org/10.1007/s11666-017-0522-0.

[57] Xie M, Zhang S, Li M. Comparative investigation on HVOF sprayed Carbide-based coatings. Appl Surf Sci. 2013;273:799–805. https://doi.org/10.1016/j.apsusc.2013.03.010.

[58] Wang H, Wang X, Song X, Liu XX, Liu XX. Sliding wear behavior of nanostructured WC-Co-Cr coatings. Appl Surf Sci. 2015;355:453–60 https://doi.org/10.1016/j.apsusc.2015.07.144.

[59] Federeci M, Menapace C, Moscatelli A, Gialanella S, Straffelini G. Pin-on-disc study of a friction material dry sliding against HVOF coated discs at room temperature and 300°C. Tribol Int. 2017;115:89–99. https://doi.org/10.1016/j.triboint.2017.05.030.

[60] Bhosale DG, Rathod WS. Tribological behaviour of atmospheric plasma and high velocity oxy-fuel sprayed WC-Cr3C2-Ni coatings at elevated temperatures. Ceram Int. 2020;46:12373–85. https://doi.org/10.1016/j.ceramint.2020.01.288.

Received 2022-02-02
Accepted 2022-03-01